

A PROCEDURE TO INVESTIGATE THE COLLAPSE BEHAVIOR OF MASONRY DOMES: SOME MEANINGFUL CASES

Milorad Pavlovic*¹, Emanuele Reccia*², Antonella Cecchi*³

*Department of Architecture Construction Conservation, University IUAV of Venezia

¹ m.pavlovic@stud.iuav.it; ² emreccia@iuav.it; ³ cecchi@iuav.it

*This is an Accepted Manuscript of an article published by Taylor & Francis in **International Journal of Architectural Heritage** on 25 Jan 2016, available at: <https://www.tandfonline.com/doi/full/10.1080/15583058.2014.951797>*

This manuscript version is made available under the CC-BY-NC-ND 4.0 license <https://creativecommons.org/licenses/by-nc-nd/4.0/>

KEYWORDS

Limit analysis, domes, masonry, crack pattern, macro model

ABSTRACT

Masonry domes represent an important part of the architectural heritage. However, the literature about domes analysis seems less consistent than the one referred to other masonry structures. The collapses happened in recent years as a consequence of seismic actions or lack of maintenance show the need of detailed studies. Here a limit analysis to evaluate the masonry domes behaviour is presented. An algorithm based on the kinematic approach has been developed to evaluate the geometric position of the hinges that determine the minimum collapse load multiplier. The proposed procedure is validated by a comparison with some meaningful cases: the collapse of *Anime Sante* Church in L'Aquila, the collapse of *San Nicolò* Cathedral in Noto, the crack pattern of *San Carlo Alle Quattro Fontane* Church in Rome and the analysis developed on *Hagia Sofia* in Istanbul. The comparison with real cases shows a good agreement between the model results and the phenomenological crack patterns.

1. WHY IS IMPORTANT TO STUDY MASONRY DOMES?

The conservation of the cultural heritage is a challenge for the contemporary society. In recent decades significant resources have been allocated for the conservation and restoration of the architectural heritage. Historical buildings were restored, protected and reinforced with the intent to limit the risks of degradation or loss, due to phenomena of structural damage and to external factors such as differential settlements, earthquake effects, etc.. The wide diffusion of historic masonry constructions in Italy, Europe and Mediterranean area requires reliable tools for the evaluation of their structural safety.

Referring to the heritage, the problem consists not only in evaluating the safety of the structure under service loads and at collapse, but also in evaluating its response to a series of hazards: variations of boundary conditions (soil settlements, induced for example by works carried out close to the construction or by groundwater level variations), structural configuration (partial demolitions, integrations and modifications, strengthening and seismic retrofitting interventions), loads (due to use variations), materials (material decay due to long-time creep effects, material improvement associated to strengthening interventions), natural hazards (earthquake, wind).

Masonry domes represent a characteristic feature of the architectural heritage. However, despite of many efforts to protect the historical heritage, during last 30 years several collapses of masonry domes occurred in Mediterranean area as a consequence of seismic actions or lack of maintenance.

For instances, the dome of the Noto Cathedral in Sicily collapsed in 1996 as a consequence of the earthquake of 1990 (Binda et al., 2003; Tringali, 2003) and more recently the same happened to the dome of Anime Sante Church after the earthquake that hit in 2009 the city of L'Aquila. Earthquakes have always been a serious hazard for this typology of structure, as demonstrated for examples by the vicissitudes of Hagia Sophia in Istanbul (Mainstone, 1988;

Hidaka *et al.*, 1993; Sato *et al.*, 1996), which has been destroyed and rebuilt many times as a consequence of seismic events.

Regardless the damages caused by earthquakes, it is common to observe cracking in masonry domes. While vertical cracks, usually do not provide problems of stability – for instances the dome of *Santa Maria del Fiore* Cathedral in Firenze have been designed by Brunelleschi considering the possibility of vertical cracking (Bartoli *et al.*,1996) – instead, horizontal cracks may be related to the development of a kinematic mechanism. An example is the church of *San Carlo alle Quattro Fontane* in Roma, built by Borromini in the seventeenth Century: the dome showed vertical cracking in the two main axis, the longitudinal and the transversal ones, and horizontal cracks at the base of the dome and at the base of the lantern (Degni, 2008).

In this paper some of the domes previously listed have been studied. They have been chosen on the base of geometrical parameters that typically may influence the structural behaviour of domes: the presence or not of the lantern, the shape – hemispheric or lowered, the plan – circular or elliptical, the presence or not of the backfill. The analyses performed have been compared with the surveys taken after the collapse, in the case of *Anime Sante* church and Noto cathedral, or with the crack pattern, in the case of *Hagia Sophia* and *San Carlo alle Quattro Fontane*.

Masonry domes are very common structures in monumental buildings that characterize the historical centres of the European cities. Although their relevance and their vulnerability, domes have not been studied as much as other masonry structures: the collapses happened in recent years show the need of detailed studies.

2. SCIENTIFIC BACKGROUND

An accurate modelling of the mechanical behaviour of masonry domes is of fundamental importance for the correct evaluation of their structural safety, hence to ensure their conservation. A dome is a vaulted structure having a circular plan and usually the form of a portion of sphere. Geometrically speaking, a dome is a surface that can be divided into a series of wedges, joined by parallel bands. Along the wedges act meridian forces which are always compressive under vertical loads, while along the parallel bands act hoop forces which are perpendicular to the meridian forces. Hoop forces, that restrain the out-of-plane movement of the wedges, are compressive in the upper zone of the dome and tensile in the lower zone, in most cases the passage from compressive to tensile forces occurs between 45 and 60 degrees respect to the vertical axis (Heymann, 1982; Como, 2011; Lucchesi, 2007), as shown in figure 1, that reports results obtained by membrane analysis of a semi-circular masonry dome (Pavlovic, 2013).

Therefore, the load bearing capacity of masonry domes is related to their shape: a dome is a double-curved shell that thanks to its shape exhibits an optimal structural behaviour under axial-symmetric loads. However, in case of masonry domes this “*shape effect*” is affected by the low tensile resistance of masonry material. When the stresses due to self-weight and dead loads exceed the weak tensile strength of masonry, first damages occur: vertical cracks open at the base of dome due to the hoop forces, it may suggest an enlargement of the drum. Due to the development of vertical cracks the dome is divided in wedges: membrane stresses become compressive stresses and the dome starts behave like a series of concentric masonry arches along the meridians. This phenomenon is quite common in masonry domes and it does not compromise their structural behaviour (Heymann, 1967; Como, 2011). Instead horizontal cracks, which are due to meridian forces, are more dangerous and may denounce the development of a kinematic mechanism that may lead to collapse. In fact, like in a simple masonry arch, the position of the line of thrust changes, moving from the centre of the section

to its hedges. When it comes out from the core of the section, the opposite side of the section is not more compressed and should transmit tensile stress, which is not allowed for masonry material. When the line of thrust touches the external or internal surface of the dome a mechanism starts: in that point a hinge develops while in the opposite side a crack opens. This kind of structure is basically designed to bear vertical dead and gravity loads only (Heymann, 1969, 1967 and 1977). For this reason masonry vaults are vulnerable to seismic actions, as enlightened in the previous section.

Although the construction of masonry domes dates back to the past, most of the domes were built before the seventeenth century, the most important studies on domes were made only starting from the eighteenth century. At that period, project was concerned the definition of geometric and material characteristics. In 1773 Coulomb has shifted the problem from planning the structure to its static verification and also introduced the concept of the friction in the mechanics of masonry structures. Thus, many following studies – Navier, Fontana, De La Hire – were developed in the same way, taking into account the friction in equilibrium questions. Many researchers were aimed at the choice of the mechanisms in agreement with the experiments conducted on various geometries of arches. Anyway, the most important structural analysis of dome made in the past is the study made by Poleni (1743) on the dome of the Basilica di San Pietro in Rome. The method proposed by Poleni to assess the stability of the San Pietro's dome – that was cracked along the meridians from the base to the lantern – was inspired by the Hooke's law and it can be considered as a first limited formulation of the static theorem of limit analysis of masonry structures (Como, 2010). A complete overview of the historical approaches to the study of arch and domes and the evolution of the structural theories may be found in Kurrer (2008).

In the first half of the twentieth century, new methods of analysis for the evaluation of the behaviour of masonry arch have been proposed. The most diffused approach to study the

stability of masonry arch has been proposed by (Pippard and Ashby, 1936; Pippard, 1948). The method, that consider the arch as a two-hinge arch for which the minimum load is applied to a fixed position, allows determining the exact position of the two additional plastic hinges that take place when the arch start behaving as a four hinges mechanism. This approach was further extended by (Heyman, 1966, 1967, 1977) whit the introduction of the line of thrust and the enunciation of the safety theorem.

Starting form the second half of the last century the attention to the domes increased: in literature numerous studies concerning the mechanical behaviour of masonry domes may be founded. Main approaches may be synthetized in simplified models and refined models. Models may be based on the limit analysis (Heymann, 1967), which are more rough but at the same time more immediate, or elastic analysis (Flügge, 1973), but also limit analysis, taking into account the mechanical properties of masonry material or the three-dimensional behaviour of domes (O'Dowyer, 1999).

Simplified models (Heyman, 1966, 1967, 1982; Oppenheim *et al.*, 1989; Livesley, 1992; Milani *et al.*, 2009a; Milani *et al.*, 2009b;) focus on the collapse of masonry domes, and are devoted to the definition of possible kinematic mechanism shapes and the evaluation of collapse load at varying loading conditions or shape of masonry domes or other geometrical parameters, such as the curvature of the dome, the presence or not of lantern and its weight, the presence of *oeil-de-boeuf* or other types of opening. The greater part of these studies follows the approach of the limit analysis, in which masonry domes are modelled as kinematic chain of rigid blocks (Gilbert and Melbourne, 1994). As well known, this modelling approach adopts for masonry material the hypotheses of infinite compressive strength, infinite sliding strength and tensile strength equal to zero, but doesn't require other specific mechanical parameters. Only few studies propose a non-linear analysis of masonry domes (Pesciullesi *et al.*, 1997; Milani and Tralli, 2012).

Other approaches focus on the elastic behaviour of masonry domes, providing more refined models, that usually represent the dome through its middle surface, fit to perform three-dimensional membrane analysis. The greater part of these models (Lucchesi *et al.*, 2007) is devoted to the definition of the stresses distribution in parallels and meridians at varying the geometrical shape of masonry dome, the loading or the boundary conditions. Masonry material is modelled as isotropic or orthotropic material depending on the sophistication of modelling approach. In so doing, mechanical parameters of blocks and mortar joints are taken into account. The sensitivity to the arrangement of blocks of the masonry domes mechanical behaviour has been widely acknowledged by historic treatises and literature (Alberti, 1989; Choisy, 1883; Nelli, 1753; Docci, 1992) and by more recent works. (Milani and Cecchi, 2013).

The present study aims to propose a simple and fast procedure to provide reliable evaluation of the minimum collapse load multiplier and of the relative mechanism of collapse, finding the position of the hinges. The method is based on the kinematic approach of the limit analysis. The use of a simplified model is justified by the fact that this typology of structure may be damaged or may collapse because of problems due to instability, without involving the strength of the masonry material. The stability of domes may easily be represented by the line of thrust and is basically related to the geometrical distribution of loads instead to the mechanical properties of masonry material, which may not be exactly established. The analysis here performed is in membrane regime, the reference is made to wedge of dome, hence a bi-dimensional analysis may be performed (Oppenheim *et al.*, 1989). This assumption is motivated by the fact that the presence of vertical cracks due to hoop forces is common in masonry domes: segmental domes do not have problem of stability (Heyman, 1977; Como, 2011; Foraboschi, 2004; Blasi *et al.*, 1994). In the case of domes subjected to uniform distributed loads, with rigid boundary conditions and in the absence of differential settlement these assumptions can be considered correct, hence it is possible to consider portion of them.

In the proposed method, domes have been divided in arches having a constant thickness. The difference in term of self-weight between arch and clove is negligible. In fact, comparing an arch having width w_A equal to 1 meter with a clove having the same width w_A of the arch at 37° (*see fig. 2*) the difference in term of volume is about 1% for domes with a thickness of 1/10 of the diameter. Moreover, the position of the centre of gravity in the arch is at 0.62 R while in the clove is at 0.48 R (*see fig. 2*): it implies an in-stabilizing effect that errs on the side of safety. The proposed method is compared with some meaningful cases of collapsed or cracked domes. The idea is to check if the position of the cracks in a masonry dome coincide with the position of the hinges related to the minimum collapse multiplier. To verify this condition, an algorithm has been developed: to define the position of the hinges that correspond to kinematic mechanism activated by the minimum collapse multiplier. The comparison between the results obtained by the limit analysis and both real crack patterns and surveys on some damaged dome allows to validate the procedure.

3. PROCEDURE TO DEFINE MINIMUM LOAD MULTIPLIER FOR LIMIT ANALYSIS

Here a method for the limit analysis based on the kinematic approach of masonry domes is presented. The proposed method has been compared with some meaningful cases of collapsed or cracked domes in order to verify its reliability. The aim is to check if the position of the cracks in a masonry dome coincides with the position of the hinges related to the minimum collapse multiplier. Hence, an algorithm has been developed; it allows to define the position of the hinges, along the intrados and the extrados, generated by a kinematic mechanism that may be activated by the minimum collapse multiplier.

3.1 GENERAL CASE

The proposed method was developed considering the section of a generic monocentric masonry dome loaded by a lantern, which weight is schematized by two symmetrical forces F_1 and F_2 equal to each other, like shown in Fig.3. For the activation of a mechanism is necessary the formation of 4 hinges. Two hinges $(X_2; Y_2)$ and $(X_4; Y_4)$ are considered fixed and the last one is supposed to be at the base of the dome, which is typical of masonry arches; the another one $(X_2; Y_2)$ is supposed to be matching the lantern. These fixed hinges are supposed to be on extrados. The position of the other two hinges $(X_1; Y_1)$ and $(X_3; Y_3)$ is considered variable along the intrados. As shown in fig. 2a, for both of them the supposed rotation is of about 70° , from the base of the dome to lantern (α_0) and from the lantern to the base (α_3). Each range has been subdivided in some significant portions and for every part have been calculated the geometric centre, the weight and the polar coordinates of the hinges. The area of every portion has been calculated like the portion of an annulus which lower and upper arches are in function of variable angles α_0 and α_3 . When the mechanism is activate the interested portions (A_1, A_2 and A_3) lose their connection and the structure collapse (see Fig.4 b).

The angle α_0 defines the portion of the dome that is not interested in the mechanism, while the A_1 is defined by the angle encompassed between α_0 and α_2 . The right part of the structure is subdivided in two portions A_2 and A_3 defined by the angle α_3 and, respectively, α_2 and α_4 . The weight of every portion is schematized by a single force applied on the centre $G_i (X_{G_i}; Y_{G_i})$ where $i = 1, 3$.

The proposed algorithm allows to define the minimum collapse multiplier in function of variable angles α_0 and α_3 . In the Table 1 is presented an application of it, regarding the geometry, presented in fig.3. The minimum collapse multiplier $\lambda_{C(\alpha_0, \alpha_3)}$, which represents the minimal horizontal force that determines the structural collapse, has been calculated in function of the variable angles α_0 and α_3 that determine not only the position of the hinges $(X_1; Y_1)$ and $(X_3; Y_3)$, but also the areas of arch portion. Each variation covers an angle from the base of the dome to the altitude of the lantern. For the left side the variation is represent by the angle α_0 , while for the right side it's schematized by the angle α_3 . The necessary condition that guarantees the minimum collapse multiplier is in function of the combination of the two angles which must respect these conditions:

$$0 < \alpha_0 < \alpha_1 \quad \text{and} \quad \alpha_2 < \alpha_3 < \alpha_4$$

$$\lambda_{C(a0, a3)} = \frac{\sum_{i=1}^n P_i \cdot \eta_i}{\sum_{i=1}^n F_i \cdot \eta_i} \quad (1)$$

where P_i is the self-loads (P_i) that represents every portion encompassed between two hinges and displacement of kinematic chain (η_i). See fig.3.

The weights of the portion of arch were calculated by:

$$P_i = A_i \cdot \gamma \quad (2)$$

where γ is the specific weight and A_i represents the area of the considered annulus. Each portion is in function of angle α_i , internal (r) and external (R) radius, while (b) and (H) are dimensions of the rectangular portion where present (i.e. an elliptic dome has a vertical part on the minor axe. See fig.3).

$$A_i = \frac{R \cdot \alpha_i + r \cdot \alpha_i}{2} \cdot (R - r) + b \cdot H \quad (3)$$

Also the positions of different centres depend of the considered portion and of the angle encompassed between two hinges. It is given by:

$$X_{G_i} = \frac{4}{3} \cdot \frac{R^3 - r^3}{R^2 - r^2} \cdot \frac{\sin \frac{\alpha_i}{2}}{\alpha_i} \cdot \cos \frac{\alpha_i}{2} \quad (4)$$

$$Y_{G_i} = \frac{4}{3} \cdot \frac{R^3 - r^3}{R^2 - r^2} \cdot \frac{\sin \frac{\alpha_i}{2}}{\alpha_i} \cdot \sin \frac{\alpha_i}{2} + \frac{H}{2} \quad (5)$$

The relative position of centres are necessary for the evaluation of the displacements (η_i), but also the position of the hinges is required. The rotation (φ_i) is considered unitary, thus:

$$\eta_{1_i} = \varphi_1 \cdot (X_{G_{1_i}} - X_{1_i}) \quad (6)$$

$$\eta_{2_i} = \varphi_1 \cdot \left(\frac{X_2 - X_{1_i}}{X_{2_{ass_i}} - X_2} \right) \cdot (X_{G_{2_i}} - X_{2_{ass_i}}) \quad (7)$$

$$\eta_{3i} = -\varphi_1 \cdot \left(\frac{X_2 - X_{1i}}{X_{2ass_i} - X_2} \right) \cdot \left(\frac{X_{3i} - X_{2ass_i}}{X_4 - X_{3i}} \right) \cdot (X_{G_3} - X_4) \quad (8)$$

$$\eta_{F_i} = -\varphi_1 \cdot (X_F - X_{1i}) \quad (9)$$

$$X_{2ass_i} = \frac{(X_4 - X_{3i}) \cdot [X_{1i} \cdot (Y_2 - Y_{1i}) + (Y_{3i} - Y_{1i}) \cdot (X_2 - X_{1i})] - X_{3i} \cdot (Y_4 - Y_{3i}) \cdot (X_2 - X_{1i})}{(Y_2 - Y_{1i}) \cdot (X_4 - X_{3i}) - (Y_4 - X_{3i}) \cdot (X_2 - X_{1i})} \quad (10)$$

$$Y_{2ass_i} = Y_1 \cdot \left(\frac{Y_2 - Y_{1i}}{X_2 - X_{1i}} \right) \cdot (X_{2ass_i} - X_{1i}) \quad (11)$$

The generic position of the hinges at intrados is obtained by:

$$X_i = \pm r \cdot \cos \alpha_i \quad (12)$$

$$Y_i = r \cdot \sin \alpha_i + H \quad (13)$$

For this generic example, represented in Fig.3, the minimum collapse multiplier $\lambda_{C(a0, a3)}$ is equal to 3.632; the combination of angles of the relative kinematic mechanism are reported in table 2.

3.2 SPECIFIC CASES

The general procedure proposed may be particularized for specific cases: i.e., in the case of hemispheric domes (see Fig.5), the term H has zero value. The forces F_1 and F_2 represent the load of the lantern. Their variation produces different values of the collapse multiplier but don't vary the position of the hinges. This means that the position of the hinges is determined by the geometry and not by the loads, while the horizontal force which determines the collapse is in function of the loads itself. For this geometric configuration the minimum collapse multiplier $\lambda_{C(a0, a3)}$ is equal to 1.113; the combination of angles of the relative kinematic mechanism are reported in table 2.

On the same way is also possible to analyze the kinematic configuration of a hemispheric dome without the lantern (see Fig.6), or an arch, on which is applied only a single force F with the aim to

simulate an eccentric load condition, instead of two like in the previous case. For this geometric configuration the minimum collapse multiplier $\lambda_{C(\alpha_0, \alpha_3)}$ is equal to 0.186; the combination of angles of the relative kinematic mechanism are reported in table 2.

3.3 CONCLUDING REMARK OF GENERAL PROCEDURE

After the calculation of the minimum collapse multipliers regarding the showed structures (Fig.3, Fig.5 and Fig.6) the results are compared in order to study the variation of the collapse multiplier and its relative variation.

The Fig.7a shows the trend of the coefficients $\lambda_{C(\alpha_0, \alpha_3)}$ in function of variable angle α_0 . The values regarding the generic case, showed in Fig.3, are significantly higher than the other two because the major stability that provides vertical portions at the base and the lantern. This values, like those of Fig. 5, have a symmetric distribution on the contrary of Fig.6, in which the hemispheric structure is loaded by an only single force and this determines more instability than the case in Fig.5.

The Fig. 7b represents the relative variation $\lambda_{C_{min}}/\lambda_{CIF_{min}}$ (where $\lambda_{C_{min}}$ is the minimum collapse multiplier of the figuration showed in fig.3, while $\lambda_{CIF_{min}}$ refers to the minimum collapse multiplier of the fig. 6) of the three minimum collapse multipliers calculated by the proposed algorithm in function of variable angle α_0 . We can see that the results obtained from the geometry proposed in the Fig.3 are almost twenty times bigger than those of the structure illustrated in Fig.6, while the configuration of Fig.5 has a value six times than Fig.6. This means that the major stability in a vaulted structure is ensured by the presence of a symmetric load (Fig.5) and also by the presence of vertical structures at the base which allows to raise the center of gravity (Fig.3).

4 SOME MEANINGFUL CASES

In this paragraph the proposed method is validated by a comparison with some meaningful cases: the map of cracks of San Carlo Alle Quattro Fontane Church in Rome, the post-collapse configuration of San Nicolò Cathedral in Noto, the post-collapse configuration of Anime Sante Church in L'Aquila, and the survey analysis made on Hagia Sofia in Istanbul. The comparison with real cases show the reliability of the method.

4.1 SAN CARLO ALLE QUATTRO FONTANE

The church of *San Carlo alle Quattro Fontane* has been planned by Borromini in Roma during the 17th Century and is one of the most famous example of Roman Baroque. The church is based on a stretched central octagonal plant flanked by lateral chapels. Several restoration work have been carried out on the whole complex during its life, but the most significant were completed only in the early 2000 (Degni, 2008). At the end of 1980's the church and the monastery were in bad state of conservation, in particular the dome showed vertical cracking in the two main axis, as shown by the survey carried out by Botta and taken from Degni (2008) reported in Fig.8.

While those cracks are typical of the masonry domes, we can observe that horizontal cracks, which characterizes kinematic mechanism, are located at the base of the dome and at the base of the lantern. Hence in the analysis two of the four hinges have been positioned in correspondence of the existing horizontal cracks, while the position of the other two hinges that develop the four hinges mechanism activated by the minimum collapse multiplier have been calculated by the proposed algorithm: they show the possible position of horizontal cracks in case of earthquake. Two models of the dome have been realized along the two main axis, because, due to the elliptic shape of the base of the dome, radius and weights are different in the longitudinal and cross sections. The weight of the lantern has been schematized by two symmetric equal forces F_1 and F_2 .

The collapse multipliers calculated along the two main axis are quite similar but not equal and so the position of the hinges are. This is due to the different angles between the base of the dome to the lantern. The minimum collapse multiplier λ_{c_i} obtained along the cross section is equal to 0.553, while on the longitudinal section λ_{c_i} is equal to 3.623; the angles related to the two minimum collapse multipliers are reported in Table 3. Fig.9 shows the two models and the kinematic mechanisms, the results obtained are compared in Fig. 10.

4.2 SAN NICOLÒ CATHEDRAL

The construction of the Noto Cathedral dates back to the 1693. The original project developed by Gagliardi was modified in 1770 after the collapse of the first dome, which occurred due to the leak

terrain strength. The reconstruction was entrusted to the architect Stefano Ittar in 1789, but also this project has not been completed because of the earthquake of 1848. The project was modified again and the dome was rebuilt for the 3rd time. During the 1950's the Cathedral was restored: maintenance operations have been carried out both on the main vertical and horizontal structures, the wooden floor has been substituted by a new one in pre-stressed concrete and the cracks of the main pillars were filled by gypsum mortar injections (Tringali, 2003). On December 13th 1990 an important earthquake hit the city of Noto: even at the moment seemed that the entity of the earthquake was insufficient to procure serious damages to the San Nicolò Cathedral, it can be stated that it was the beginning of a series of phenomena of instability that led to the collapse of the dome on March 13th 1996. The collapse is certainly to be attributed to a number of weaknesses and injuries suffered by the structures as a consequence of the earthquake of 1990, but also the low quality of the masonry material and presence of the pre-stressed concrete slab was crucial in the collapse of the dome (Binda et al., 2003). In fact, the heavy loads of the concrete slab were transmitted to the pillars – which have been partially damaged during the earthquake – leading to their collapse that involved parts of the roof of the dome (Como, 2010). The conservation state of the Cathedral after the collapse is reported in Fig.11.

The analysis performed shows a good agreement between the kinematic mechanism of collapse obtained and the damages occurred during the collapse (see Fig.12). It is possible to observe that the damages interested a big portion of the dome (bigger than the Anime Sante collapse), probably due to the incompatibility of the materials: when the earthquake occurred the concrete slab had a different structural behaviour than the other masonry structures and it produced horizontal forces at the base of the dome. In the analysis a hinge has been assumed in correspondence of that point. The minimum collapse multiplier and the angles that determine the position of the hinges of the relative mechanism – reported in Table 3 – are compatible with the real situation.

4.3 ANIME SANTE CHURCH

The construction of the Anime Sante Church begun in 1713 to commemorate the victims of the earthquake that destroyed the city of L'Aquila in 1703. The church consists of a rectangular hall with a

barrel vault flanked by two chapels on each side, with eight windows placed to illuminate the presbytery from the hemispherical dome (see Fig.13). On April the 6th 2009 an earthquake of $M_w = 6.3$ ($M_L = 5.8$) hit L'Aquila and dozens of villages along the Aterno valley. The earthquake caused 308 victims and seriously damaged the historic centre of L'Aquila. The Anime Sante Church had the same destiny: the earthquake provoked the collapse of the lantern and of the dome, diffused cracks of the key stone arches, detachment of the façade and apse and shear cracking of several walls (see Fig.14).

The analysis has been performed considering the hemispheric portion of the dome loaded by two equal symmetric forces F_1 and F_2 to simulate the lantern. The lowest collapse multiplier λ_{c_i} is equal to 0.077 and is provided by the kinematic chain illustrated in Fig.15. The mechanism of collapse is shown in Fig.16 together with a modal analysis performed by means of Finite Element in membrane regime. The first natural frequency corresponds to a local mode of vibration of the lantern, hence, during the seism, stresses were concentrated at the base of it leading to a local mechanism that caused the collapse of the lantern itself. Looking at the surveys carried out after the earthquake (see Fig.14) it clearly appears that the lantern was the first element that collapsed dragging a portion of the dome: the results of the limit analysis are in good agreement with it, as shown in Fig.16.

A further limit analysis has been performed taking into account the backfill at the base of dome, which provides a stabilizing effect (Reccia *et al.*, 2014). The analysis has been performed starting from the results obtained without backfill: the combination of angles that provides the minimum collapse multiplier has been used to calculate the variation of the minimum collapse multiplier considering the backfill. Once determined geometry, weight (P_{i_rin}) and barycentre (X_{G_rini} ; Y_{G_rini}) of the backfill, the relative horizontal ($\delta_{_rini}$) and vertical ($\eta_{_rini}$) shifts have been calculated in order to find the minimum collapse multiplier (see Fig.17). The collapse multiplier obtained considering the backfill is significantly bigger than the previous: $\lambda_{c_rin} = 0.302$, hence the backfill provide an increase of stability equal to about 23%, as shown in Fig.18, where results are compared; the values of multipliers and angles are reported in Table 3.

4.4 HAGIA SOFIA

Hagia Sophia was originally built in the fourth Century under Constantine, but soon after was totally destroyed by an earthquake. In the sixth Century it was rebuilt by Emperor Justinian but collapsed again during another earthquake in 558. The dome was then rebuilt in the 562 with a greater height (Mainstone, 1988), giving Hagia Sofia the actual configuration (apart from the minarets made in the sixteenth Century when it was transformed into a mosque). Afterwards, in the course of its history, several collapses occurred, with different reconstructions: the western arch was damaged during the earthquake of 869, while the western part of the dome collapsed during that of the 989. The earthquake of 1346 provoked a further collapse of the dome, damaging about one-third of the area opposite to the one that collapsed of the 989. The reconstruction of this portion (see Fig.19), which ended a few years later, still shows the discontinuity between the reconstructed area and the pre-existing. In the following centuries did not happen further collapses, however the dome is weakened by the lack of homogeneity between the three portions which is constituted by and by the strong irregularities in the whole geometry (Hidaka et al., 1993; Sato et al., 1996).

The structure of the church is complex. The great dome, 34 m of diameter, is supported by a system of four pillars and six arches: it was the first example in which were used the so called *pendentives* to join the rectangular base to the hemispheric dome. The stability of the dome is ensured by two different structural systems: in the longitudinal section (East - West) there are two semi-domes that contrast the weight and the thrust of the dome, while in the cross section (North-South) the same task is given by a system of buttresses, which produce a passive way of stability (see Fig.20).

The analysis has been carried out on the base of the surveys and studies of Mainstone (1988): both the original and the rebuilt domes have been analysed. Fig.21 and Fig. 23 shows the two mechanisms of collapse: the rebuilt dome has a greater stability than the original one. It is also possible to notice that the first hinge coincides with the existing buttress at the base of the dome, that should provide an increase of stability. A further analysis of the two domes has been performed taking into account them. Similarly to what previously done in the analysis of Anime Sante, the geometry, weight (P_{i_rin}) and barycentre (X_{G_rini} ; Y_{G_rini}) of the buttress, the relative horizontal (δ_{rini}) and vertical (η_{rini}) shifts have been calculated in order to find the minimum collapse multiplier (see Fig.24). Also in this case, the collapse multipliers obtained considering the backfill are significantly bigger than the previous

ones, as shown in Fig.25. This means that the buttress' guarantee a major stability of the whole structure, even if they're made of different material because the stability is insured by the position of the centre of gravity. The results are compared in Fig.25, the values of multipliers and angles are reported in Table 3.

5 CONCLUSIONS

Limit kinematic analysis may be a reliable procedure to investigate the behaviour at failure of historical masonry domes. The algorithm here presented provides a fast and reliable estimations of collapse multiplier and mechanism of collapse, as demonstrated by the comparison with some meaningful real cases. The analyses conducted in this work, if considered synoptically, allow to outline the following remarks on the cases of study analysed:

- 2D analyses are suitable to evaluate the collapse behaviour of masonry domes, the 3D effect may be neglected for the evaluation of the minimum collapse multiplier. However, when needed, 2D limit analysis may be coupled with more complex analysis able to take into account the mechanical characteristics of materials and the 3D effect.
- The lantern is an essential element of masonry dome, which play an important role in the structural behaviour of domes.
- Backfill and buttress increase the stability of masonry domes.

The conservation of masonry dome may be improved thanks to a fast and reliable tool of analysis such as the algorithm here presented, if combined with proper engineering reasoning.

REFERENCES

- Alberti, L.B. 1989 *L'architettura*. Traduzione di Giovanni Orlandi, Introduzione e note di Paolo Portoghesi, Milano, Il Polifilo.
- Bartoli, G., A. Chiarugi, and V. Gusella. 1996. Monitoring Systems on Historic Buildings: The Brunelleschi Dome. *Journal of Structural Engineering* 122 (6): 663-673.
- Binda, L., Tiraboschi, C. and Baronio G. 2003 On-Site Investigation on the Remains of the Cathedral of Noto. *Construction and Building Materials* 17 (8): 543-555.
- Blasi, C., Foraboschi, P. 1994 Analytical approach to collapse mechanisms of circular masonry arch. *Journal of Structural Engineering*, 120 (8): 2288-2308.
- Choisy, A. 1883 *L'art de batir chez les Byzantins*, Parigi.
- Como, M. 2010 *Statica delle costruzioni storiche in muratura*. Roma, Aracne Editrice.
- Degni, P. 2008 *La "fabbrica" di San Carlino alle Quattro Fontane: gli anni del restauro*, Roma, Istituto poligrafico e Zecca dello Stato.
- Docci, M. 1992 La geometria delle cupole sangallesche a spinapesce in *Saggi in onore di Renato Bonelli*, edited by Bozzi, G., Carbonara, G., Villetti, G., in *Quaderni dell'Istituto di Storia dell'Architettura, Università degli Studi di Roma la Sapienza* 15-20, Roma, Multigrafica Editrice.
- Flügge, W. 1973 *Stresses in shells*. Berlin, Springer & Verlag.
- Focacci, F. 2008 *Rinforzo delle murature con materiali composite*. Palermo, Dario Flaccovio Editore.
- Foraboschi, P. 2004 Strengthening of masonry arches with fiber-reinforced polymer strips. *Journal of Composites for Construction*, 8 (3): 191-202.
- Gilbert, M., Melbourne, C. 1994 Rigid block analysis of masonry structures, *Structural*

Engineering, 72 (21): 356-361.

Heyman, J. 1966 The Stone Skeleton. *International Journal of Solids and Structures*, 2: 249-279.

Heyman, J. 1967 On shell solutions of masonry domes. *International Journal of Solids and Structures*, 2: 227-240.

Heyman, J. 1977 *Equilibrium of shell structures*. Oxford, Clarendon Press.

Heyman, J. 1982 *The masonry arch*. Chichester, Ellis Horwood

Hidaka, K., Sato, T., Kawabe, Y., Yorulmaz, M. 1993 Photogrammetry of the eastern semi-Dome of Hagia Sophia, Istanbul”, *Proceedings of the IASS-MSU International Symposium on “Public Assembly Structures from Antiquity to the Present”*, Istanbul, Turkey, 24-28 May 1993, Ed. Mimar Sinan Universitesi, Istanbul.

Kooharian, A. 1953 Limit Analysis of voussoir (segmental) and concrete arches, in *Proc. Am. Conc. Ins.*, 49: 317-328

Kurrer, K.E. 2008 *The history of theories of structures. From arch analysis to computational mechanics*. Berlin: Ernst and Son.

Livesley, R.K. 1992 A computational model for the limit analysis of three-dimensional masonry structures, *Meccanica*, 27 (3): 161-172.

Lucchesi, M., Padovani, C., Pasquinelli, G., Zani, N. 2007 Static analysis of masonry vaults, constitutive model and numerical analysis, *Journal of Mechanics of Materials and Structures* 2 (2): 221–244.

Mainstone, R. J. 1988 *Hagia Sophia, architecture, structure and liturgy of Justinian's great church*. New York, Thames and Hudson.

Milani, G., Cecchi, A. 2013 Compatible model for herringbone bond masonry: Linear elastic

homogenization, failure surfaces and structural implementation. *International Journal of Solids and Structures*, 50 (20-21): 3274-3296.

Milani, G., Milani, E., Tralli, A. 2009a Upper Bound limit analysis model for FRP-reinforced masonry curved structures. Part I: Unreinforced masonry failure surfaces, *Computers and Structures*, 87: 1516-1533.

Milani, G., Milani, E., Tralli, A. 2009b Upper Bound limit analysis model for FRP-reinforced masonry curved structures. Part II: Structural Analyses. *Computers and Structures*, 87,: 1534-1558.

Milani, G., Tralli, A. 2012 A simple meso-macro model based on SQP for the non-linear analysis of masonry double curvature structures. *International Journal of Solids and Structures*, 49 (5): 808-834.

Nelli, G.B. 1753 Ragionamento sopra la maniera di voltar le cupole senza adoperarvi le centine, *Discorsi di Architettura*. Firenze.

Oppenheim, I.J., Gunaratnam, D.J., Allen, R.H. 1989 Limit state analysis of masonry domes. *Journal of structural engineering*, 115 (4): 868-882.

O'Dowyer, D. 1999 Funicular analysis of masonry vaults. *Computer and Structures*, 73: 187-197.

Pavlovic, M., 2013 Alcune considerazioni sulle cupole storiche, *Tecnologos*, 24, ISSN 1721-6977

Pippard, A.J.S. 1948 The approximate estimation of safe loads on masonry bridges. *Civ Eng War: Inst Civ Engrs*, 1: 365.

Pippard, A.J.S., Ashby, E.R.J. 1936 An experimental study of the voissour arch. *J Inst Civ Engrs*, 10: 383–403.

Pesciullesi, C., Rapallini, M., Tralli, A., Cianchi, A. 1997 Optimal Spherical Masonry Domes of Uniform Strength. *Journal of Structural Engineering*, 123 (2): 203-209.

Poleni, G.B. 1748 *Memorie istoriche della gran Cupola del Tempio Vaticano*, Padova.

Reccia, E., Milani, G., Cecchi, A., Tralli, A. 2014 Full 3D homogenization approach to investigate the behaviour of masonry arch bridges: The Venice trans-lagoon railway bridge, submitted

Sato, T., Hidaka, K., Kawabe, Y., Aoki, T., Yamashita, K. 1996 Formal Characteristics of the setting lines on the cornice of the main Dome of Hagia Sophia, Istanbul, *J. Arch. Plann. Environ. Eng., Alj*, n. 485, July 1996.

Tringali, S. 2003 The partial reconstruction design of the Cathedral of Noto - part I: The social-economic impact on the town and on the territory and the cross-vaults, arches and dome system. *Construction and Building Materials*, 17 (8): 595-602.

LIST OF CAPTION

Fig.1 – Membrane analysis performed on Hagia Sophia dome:

a) stresses along parallels; b) comparison between meridian and hoop stresses.

Fig.2 – Comparison between clove and slice.

Fig.3 – General case.

Fig.4 – Angles (a) and portions (b) considered.

Fig.5 – Monocentric dome with lantern

Fig.6 – Monocentric dome loaded by single force

Fig.7 – Comparison between the minimum collapse multipliers (a) and their relative variation (b)

Fig. 8 – Crack pattern of the dome of San Carlo alle Quattro Fontane (Degni, 2008)

*Fig. 9 – San Carlo alle Quattro Fontane, mechanisms of collapse:
longitudinal section (a) and cross section (b).*

*Fig.10 – San Carlo alle Quattro Fontane: comparison between collapse multipliers along main axes:
cross section (SS) and longitudinal section (SL)*

Fig.11 – The Cathedral of Noto after the collapse of the dome

Fig. 12 – Kinematic analysis and collapse simulation of the Cathedral of Noto.

Fig. 13 – Anime Sante Church before the earthquake

Fig. 14 – Anime Sante Church after the earthquake

Fig. 15 – Anime Sante kinematic alarm

Fig. 16 – Anime Sante collapse simulation:

(a) Modal analysis; (b) mechanism of collapse

Fig. 17 – Anime Sante: collapse simulation taking into account the backfill.

Fig. 18 – Anime Sante: comparison of results considering or not the backfill;

(red without backfill; blue with backfill).

Fig. 19 – Hagia Sophia: crack pattern (a) and reconstruction (b), taken from Mainstone (1988).

Fig. 20 – Hagia Sophia: figure taken from Mainstone with defined structural scheme (1988).

Fig. 21 – Hagia Sophia: mechanism of collapse of the original dome.

Fig. 22 – Hagia Sophia: mechanism of collapse of the original dome with backfill.

Fig. 23 – Hagia Sophia: mechanism of collapse of the rebuilt dome.

Fig. 24 – Hagia Sophia: mechanism of collapse taking into account the backfill.

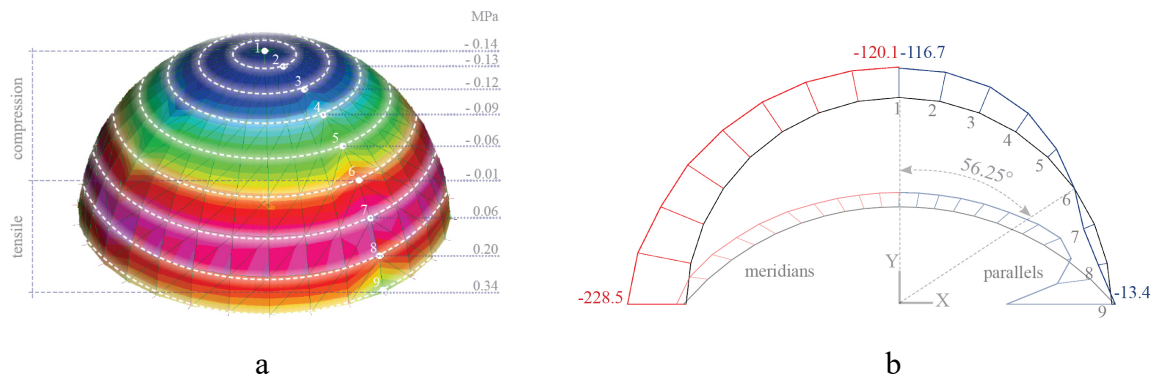
Fig. 25 – Hagia Sophia: comparison between the original and the rebuilt dome considering or not the backfill.

Table 1 – Example of algorithm's calculation.

Table 2 – Angles (rad) and minimum collapse multiplier of the different schematization of dome.

Table 3 – Angles (rad) and minimum collapse multipliers for the different cases study.

FIGURES



*Fig.1 – Membrane analysis performed on Hagia Sophia dome:
a) stresses along parallels; b) comparison between meridian and hoop stresses.*

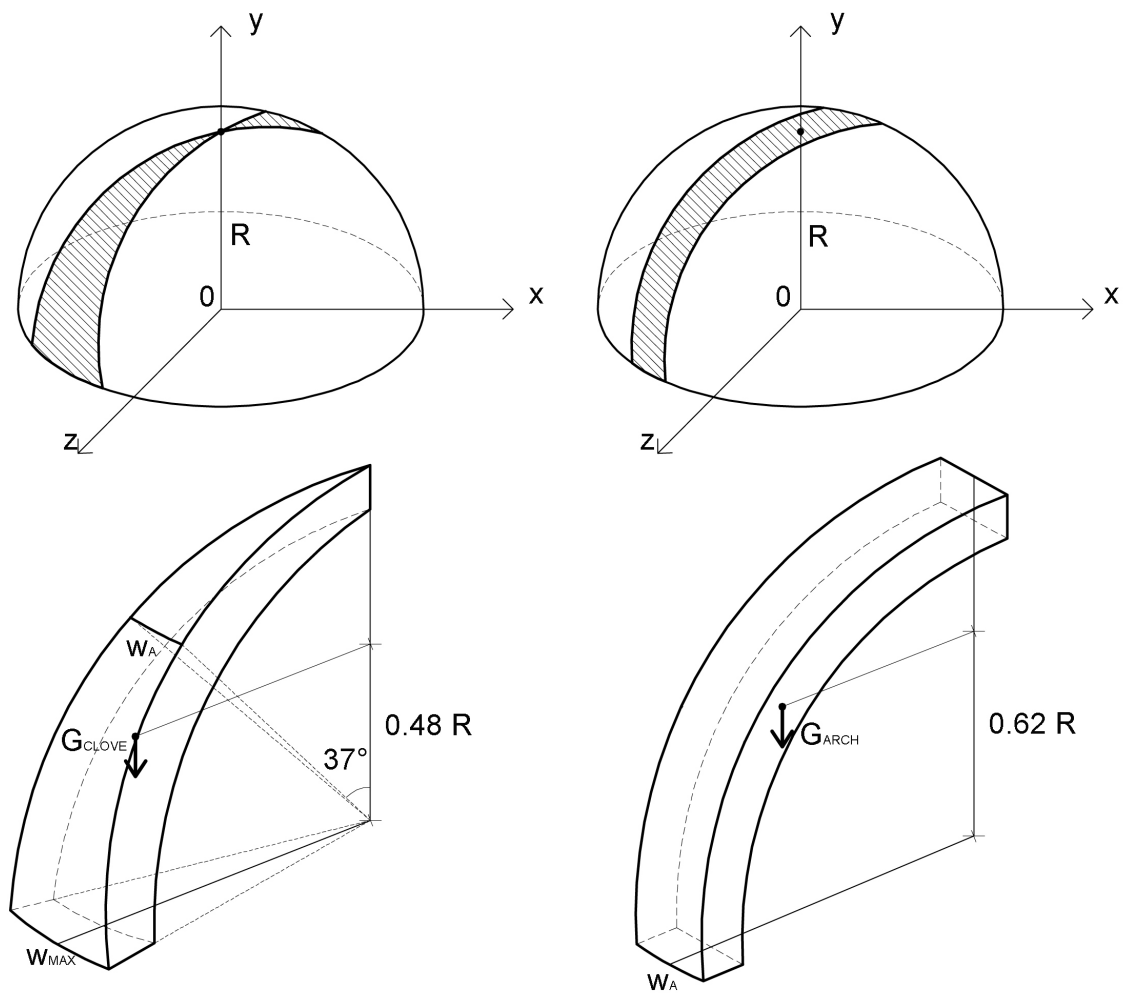


Fig.2 – Comparison between clove and slice.

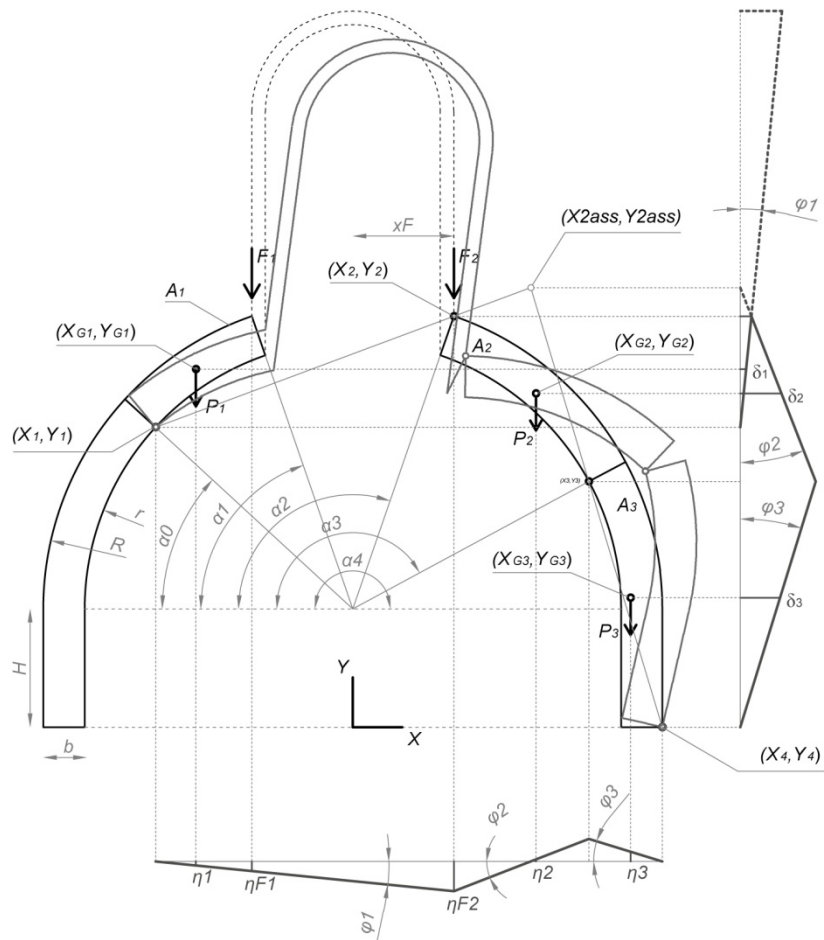


Fig.3 – General case.

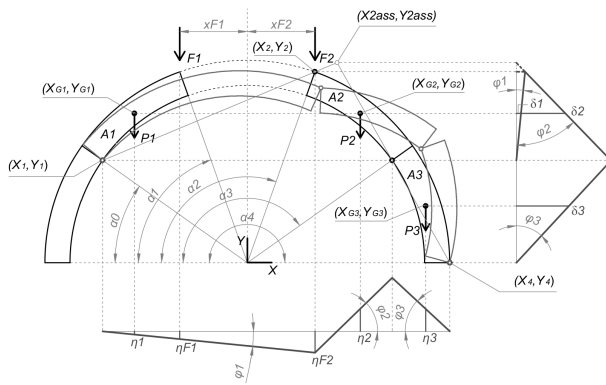


Fig. 5 – Mono-centric dome with lantern

single force

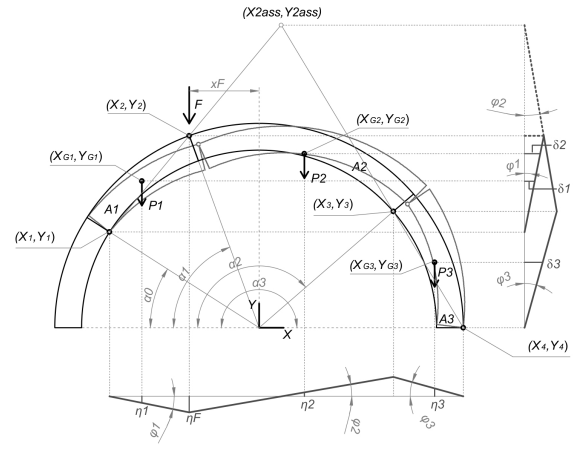


Fig. 6 – Mono-centric dome loaded by

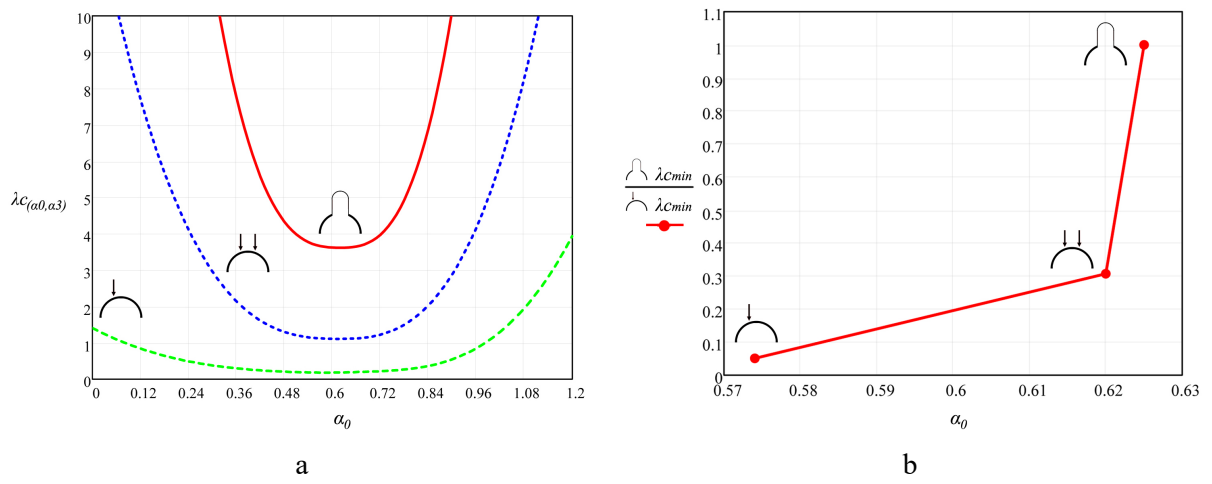


Fig.7 – Comparison between the minimum collapse multipliers (a) and their relative variation (b)

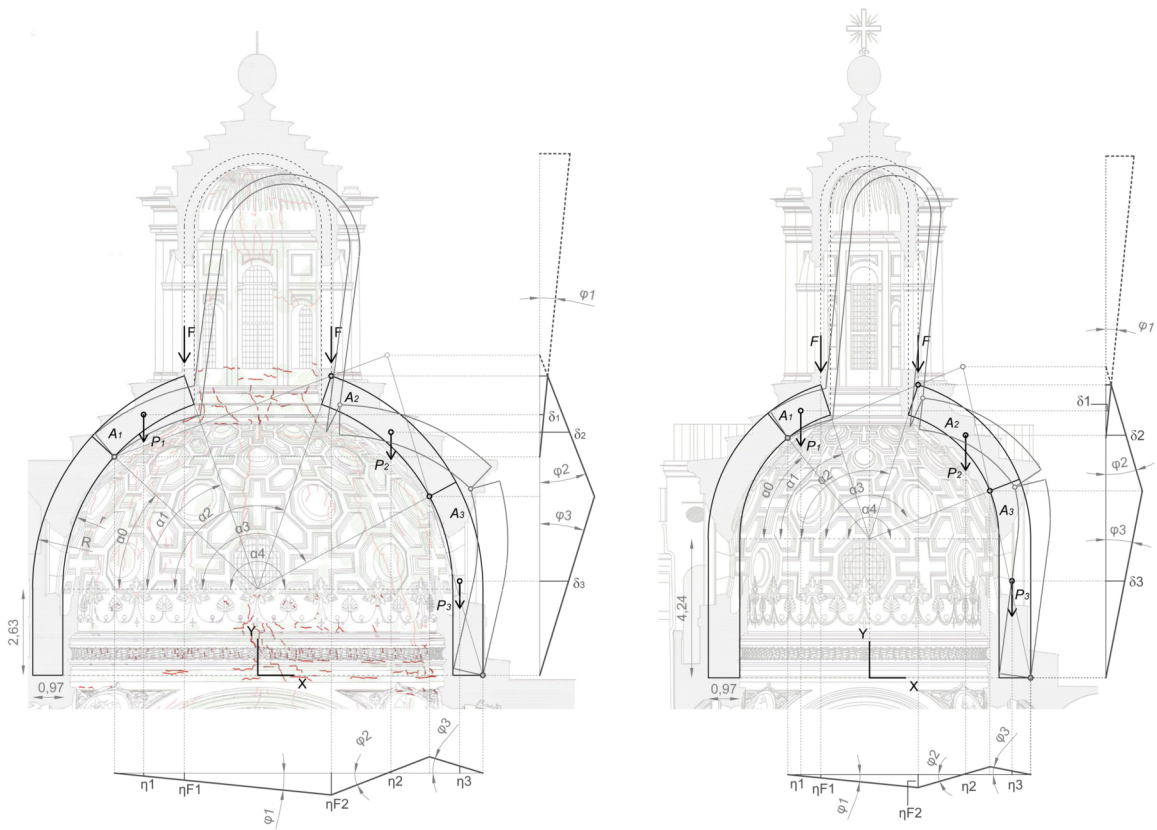
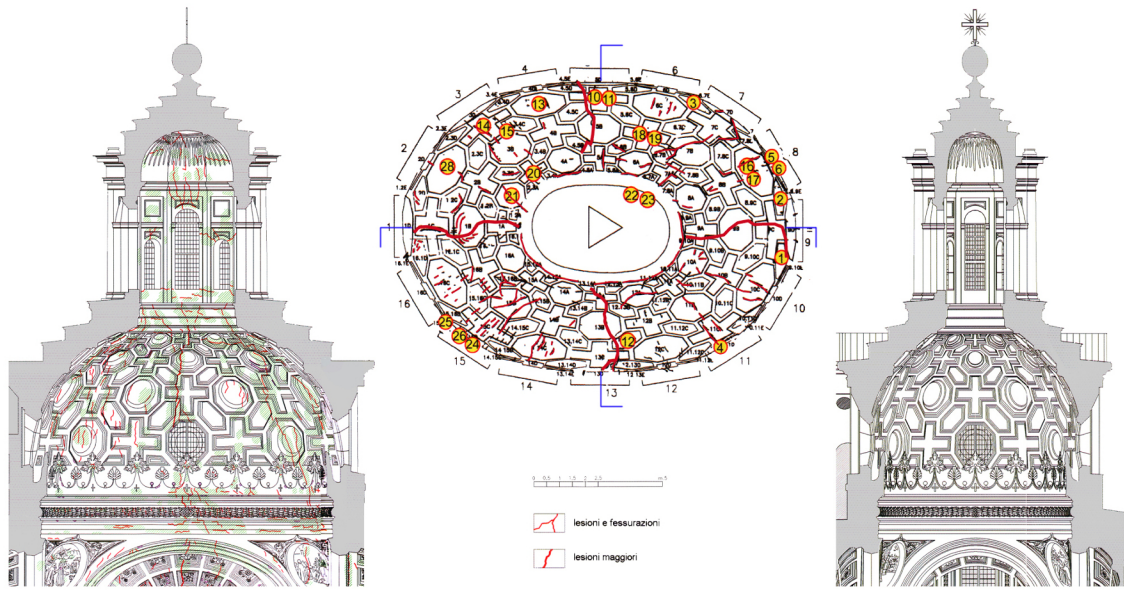


Fig. 8 – Crack pattern of the dome of San Carlo alle Quattro Fontane (Degni, 2008)

a

b

Fig. 9 – San Carlo alle Quattro Fontane, mechanisms of collapse: longitudinal section (a) and cross section (b).

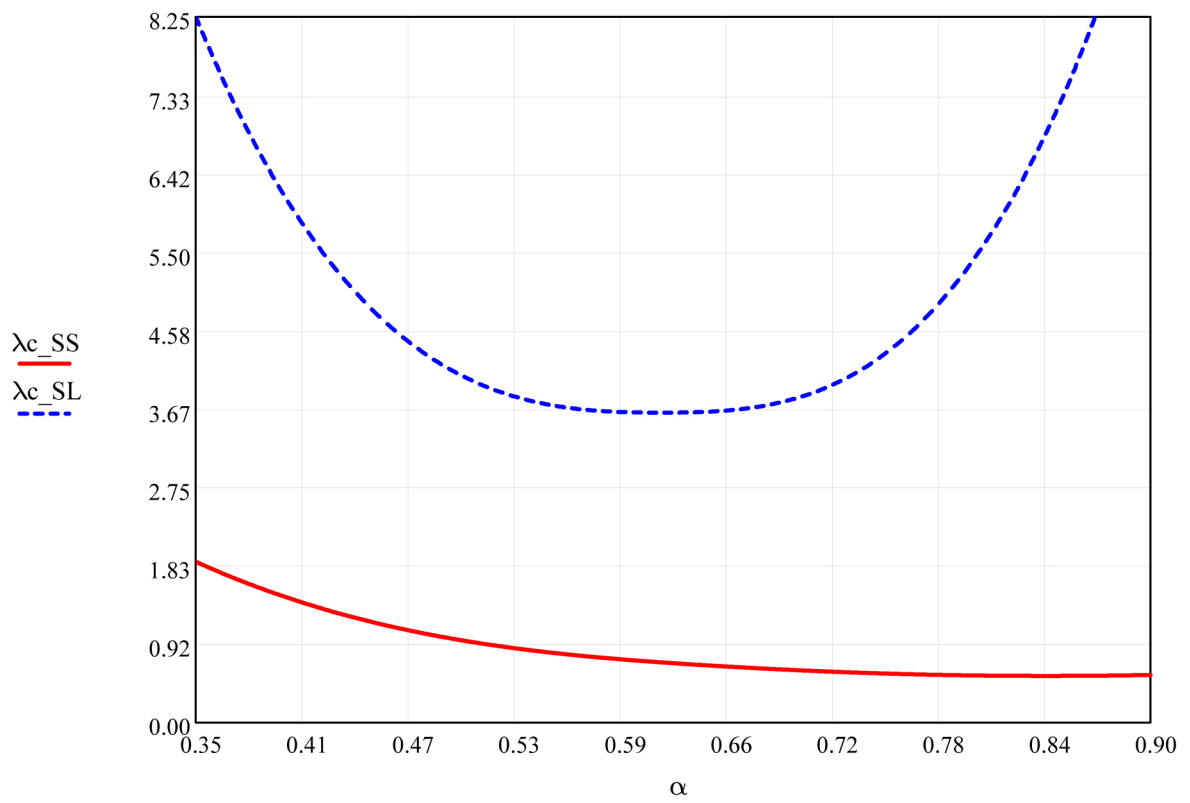


Fig.10 – San Carlo alle Quattro Fontane: comparison between collapse multipliers along main axes: cross section (SS) and longitudinal section (SL)



Fig.11 – The Cathedral of Noto after the collapse of the dome

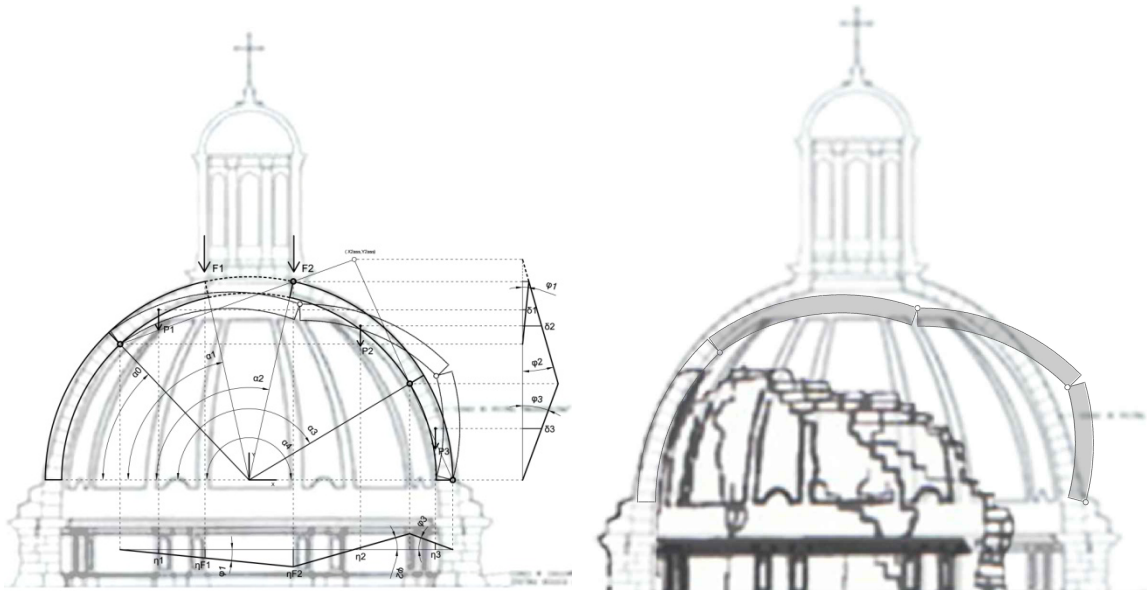


Fig. 12 – Kinematic analysis and collapse simulation of the Cathedral of Noto.



Fig. 13 – Anime Sante Church before the earthquake

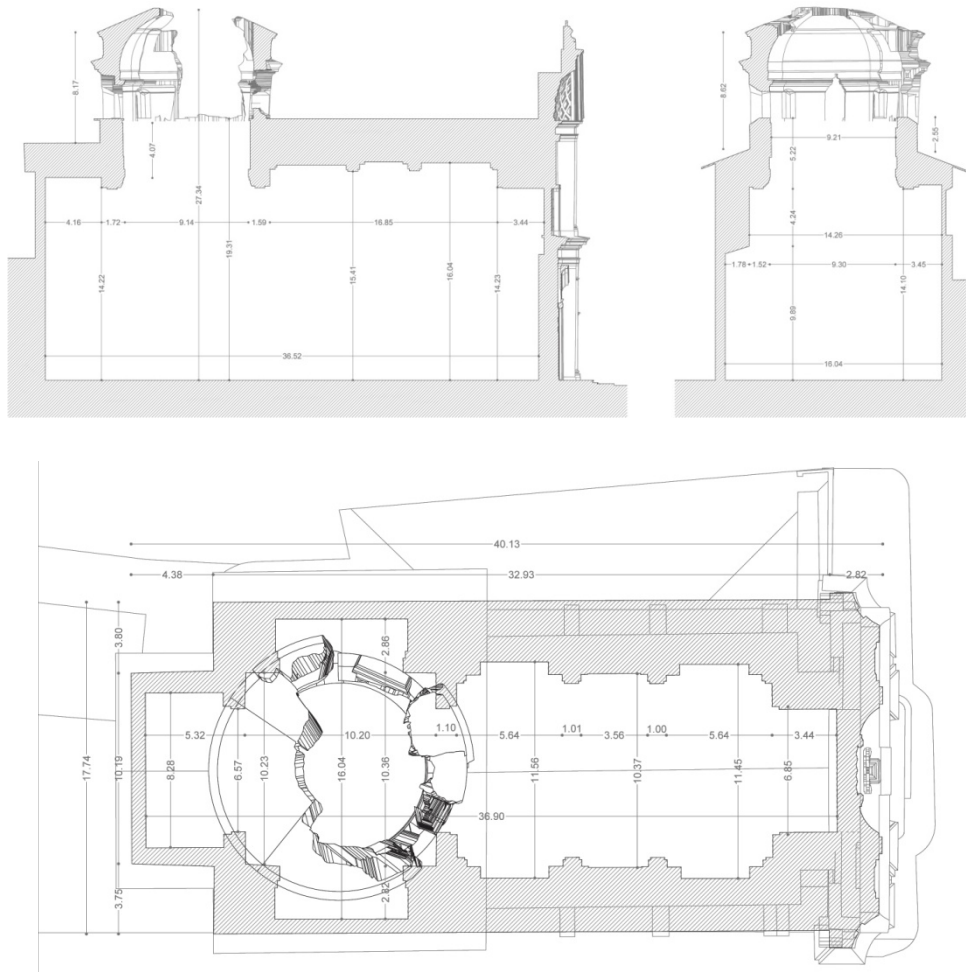


Fig. 14 – Anime Sante Church after the earthquake

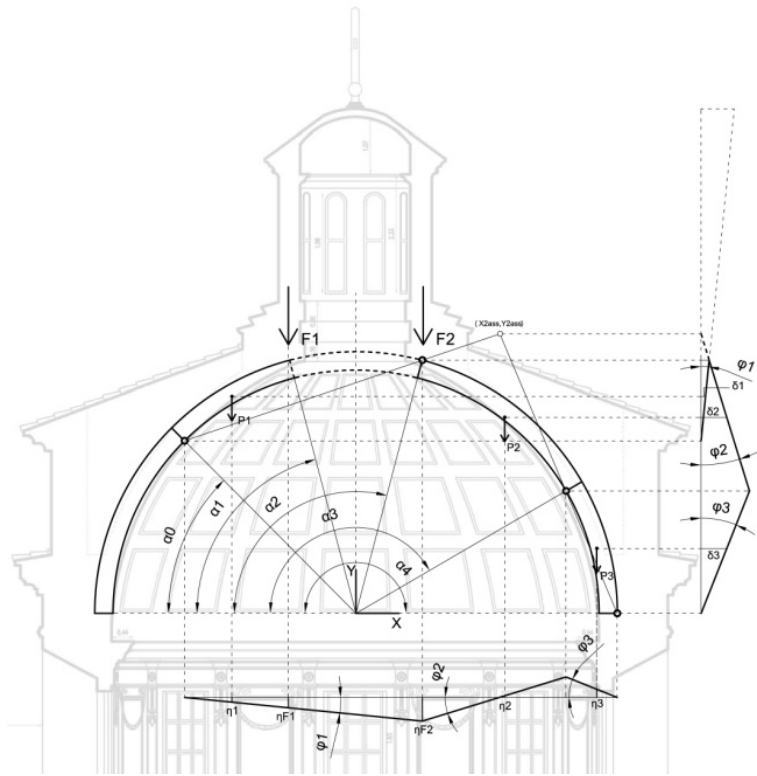
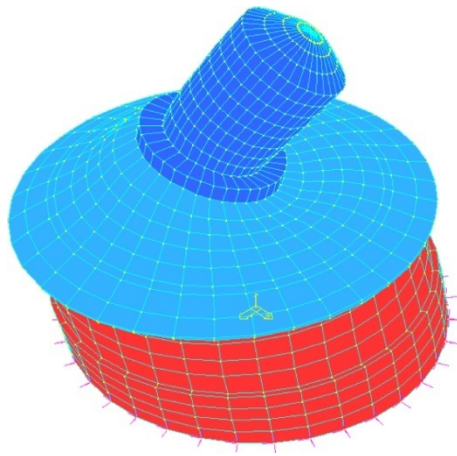
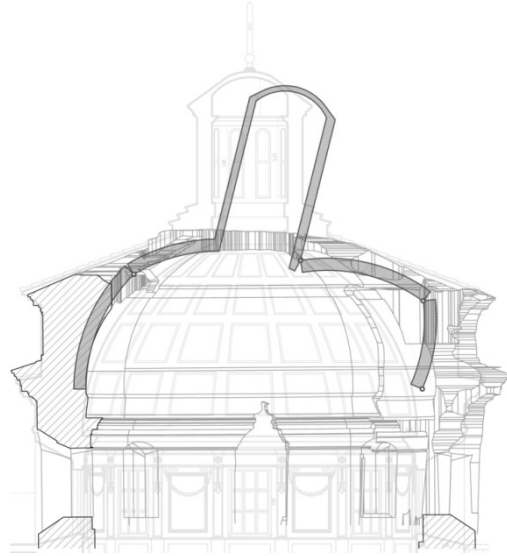


Fig. 15 – Anime Sante kinematic alarm



a



b

*Fig. 16 – Anime Sante collapse simulation:
(a) Modal analysis; (b) mechanism of collapse*

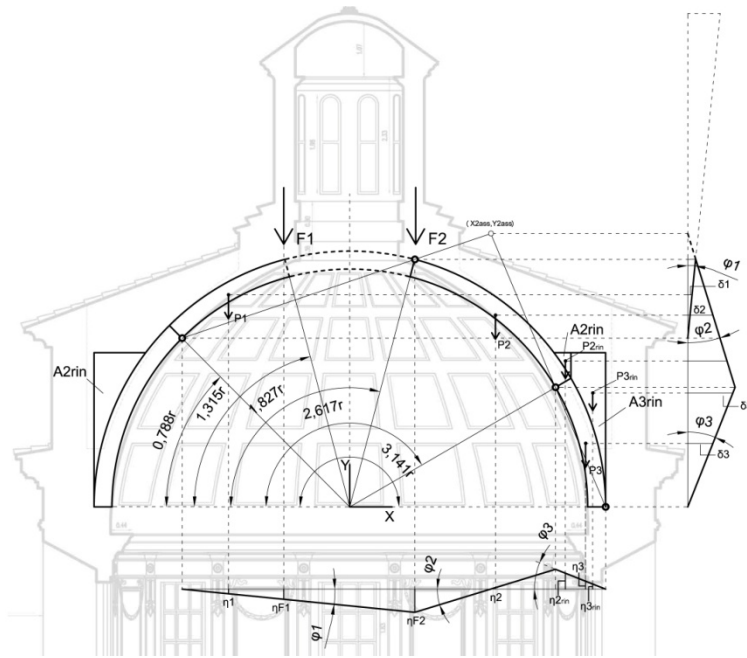


Fig. 17: Collapse simulation of the Anime Sante dome taking into account the backfill.

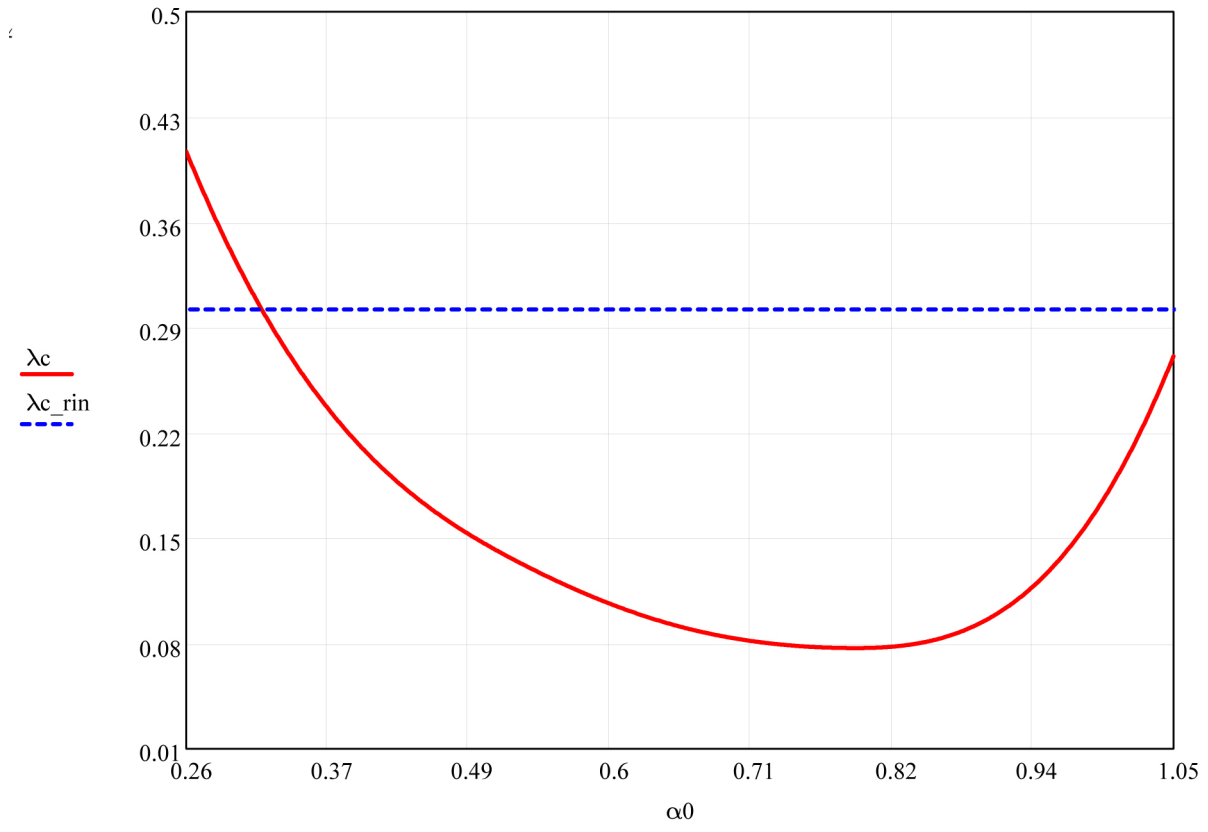


Fig. 18 – Anime Sante: comparison of results considering or not the backfill; (red without backfill; blue with backfill).

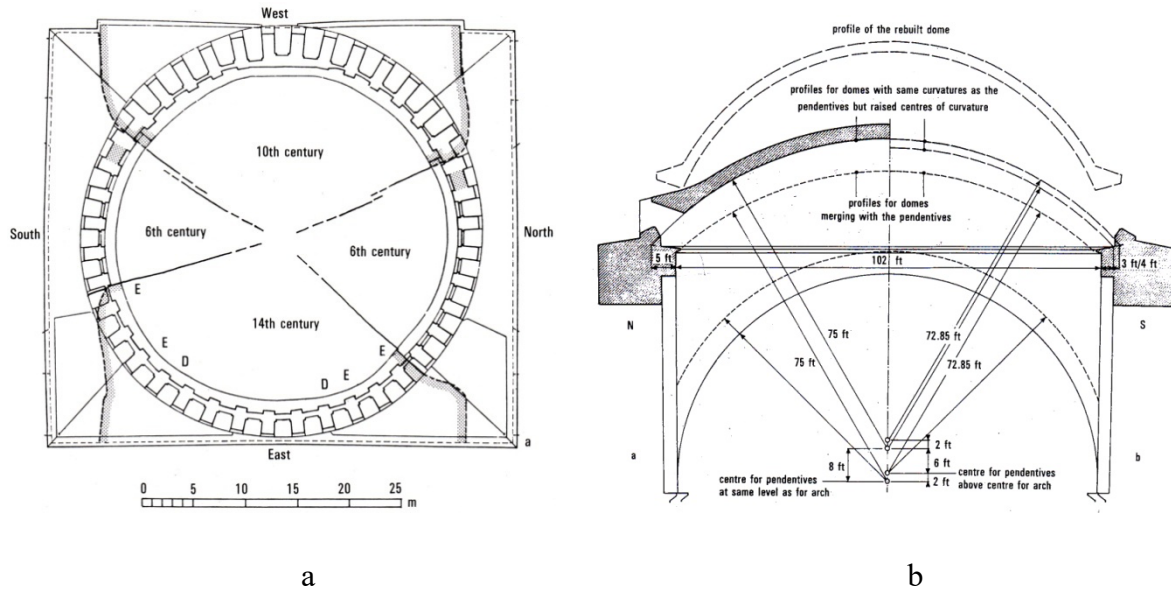


Fig. 19—Hagia Sophia: crack pattern (a) and reconstruction (b), taken from Mainstone (1988).

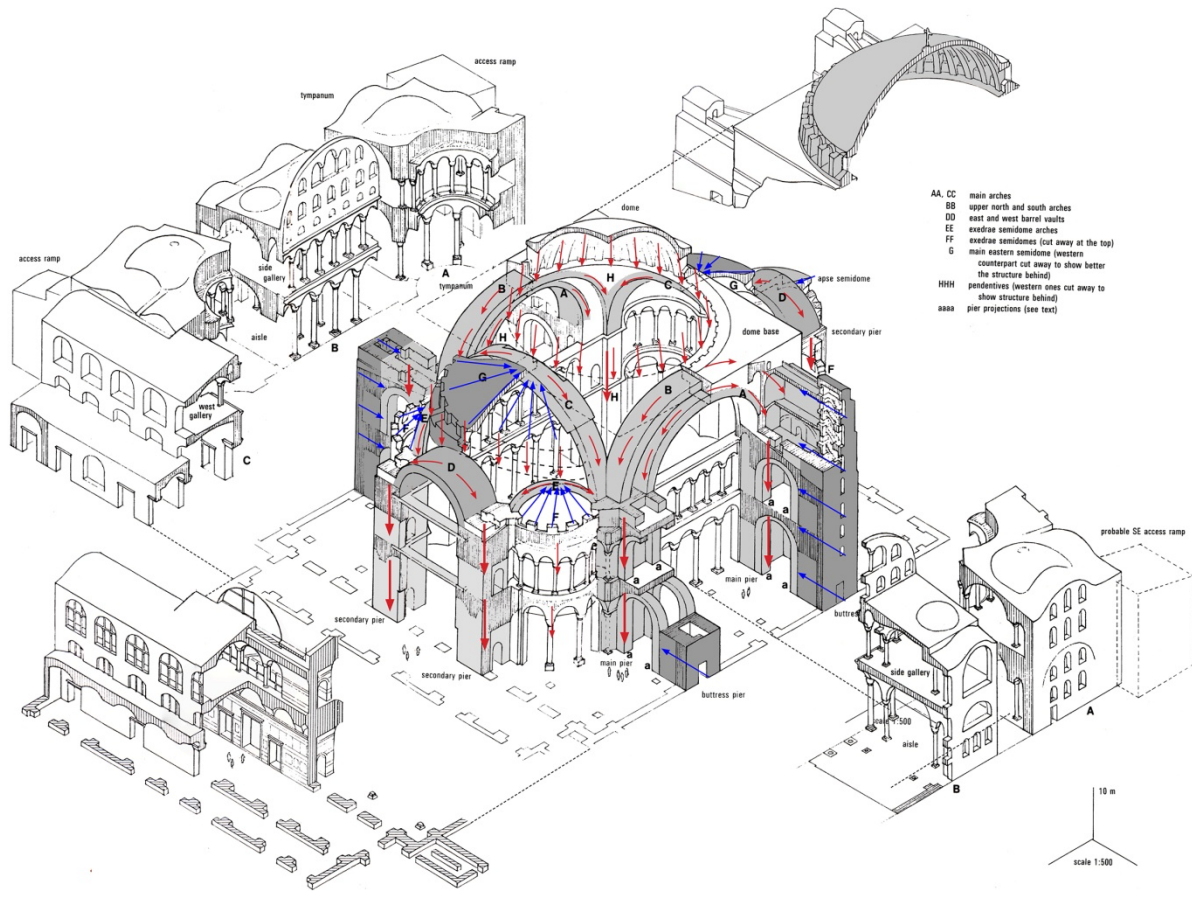


Fig. 20 – Hagia Sophia: figure taken from Mainstone with defined structural scheme (1988).

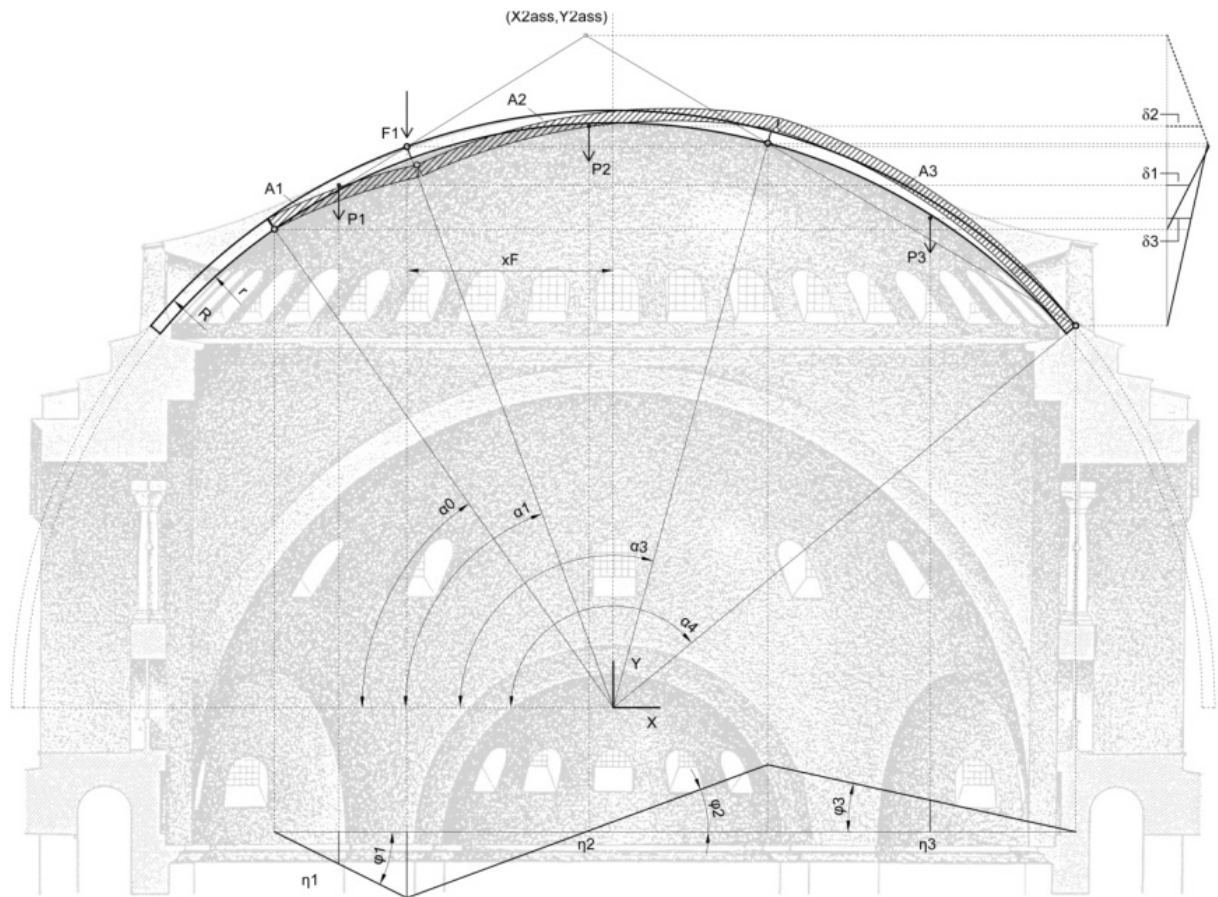


Fig. 21 – Hagia Sophia: mechanism of collapse of the original dome.

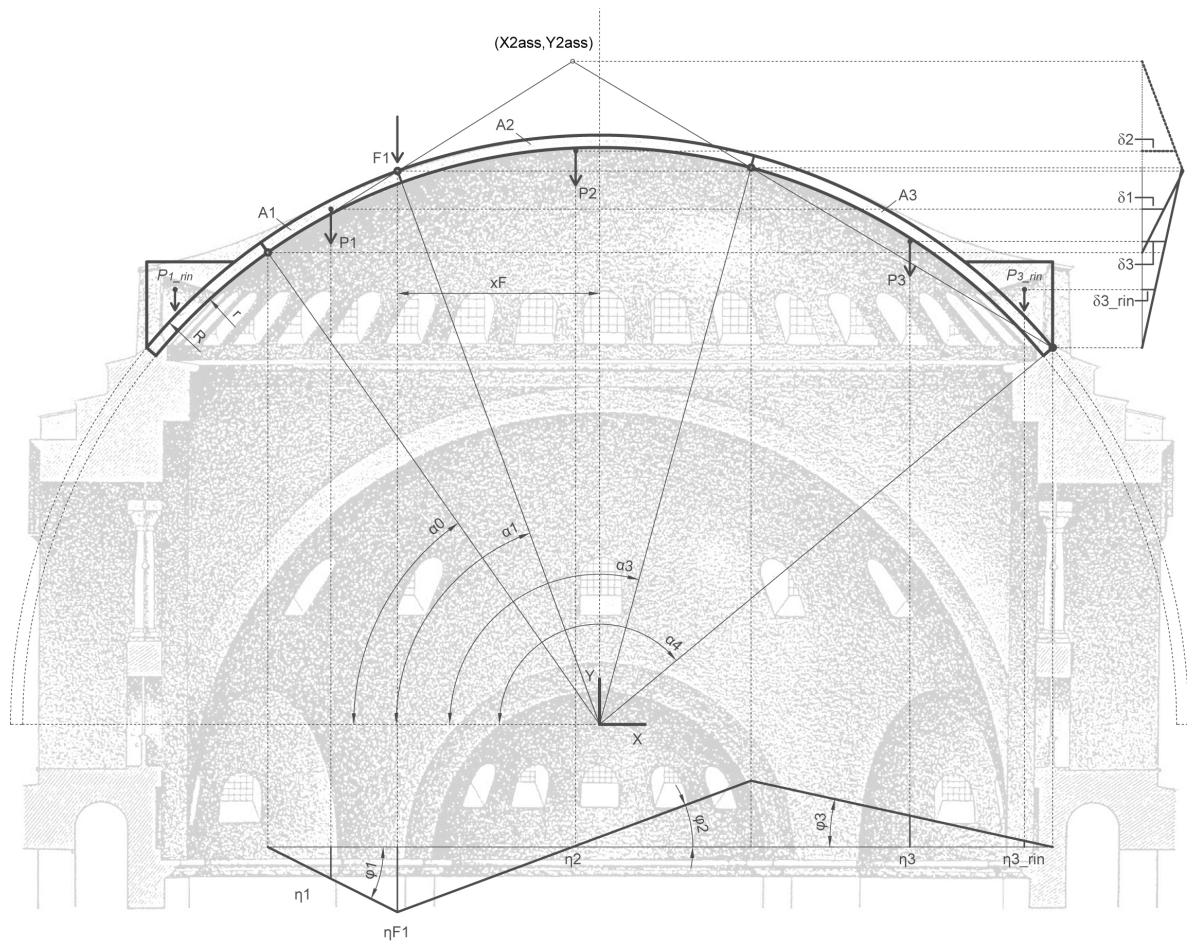


Fig. 22 – Hagia Sophia: mechanism of collapse of the original dome with backfill

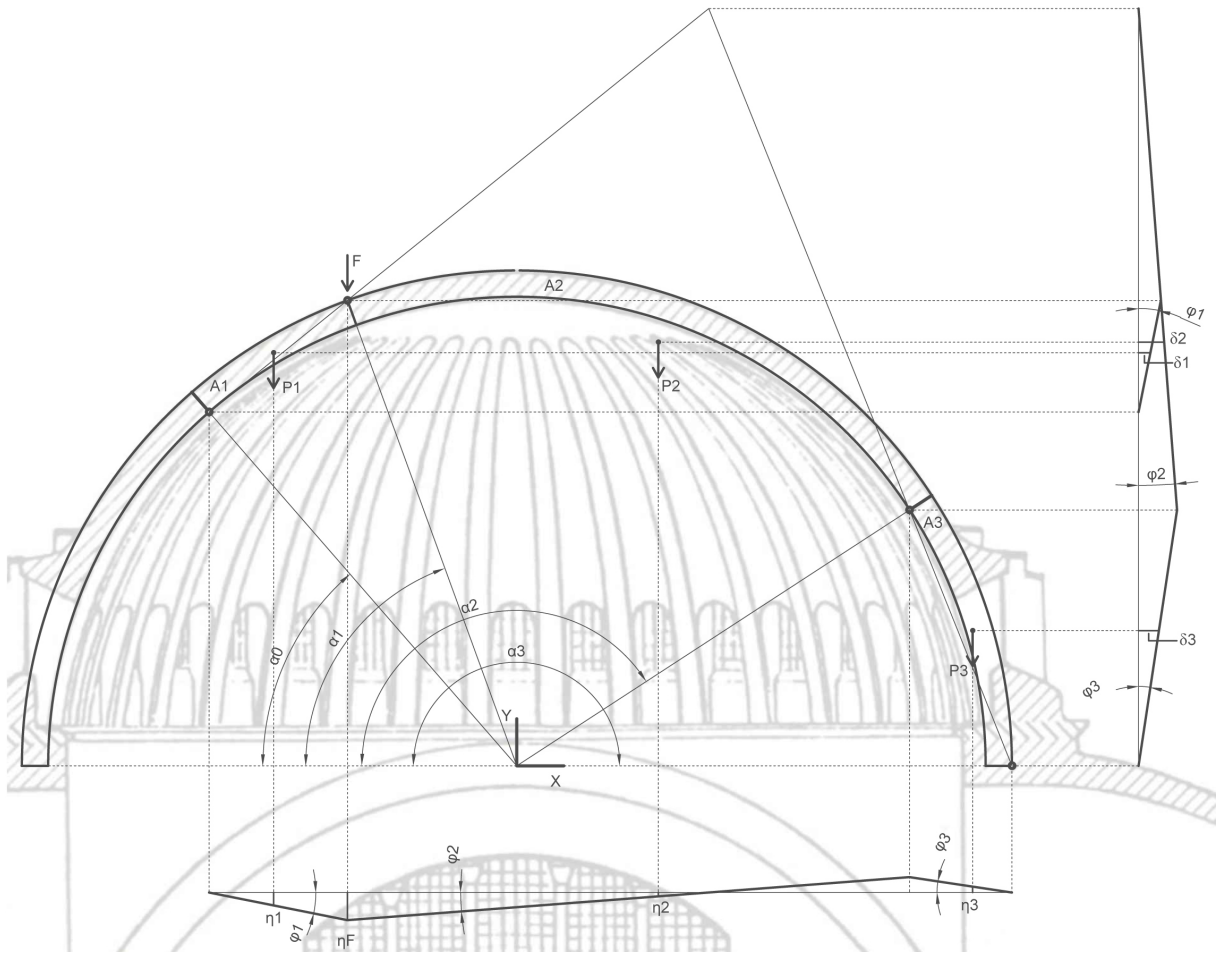


Fig. 23 – Hagia Sophia: mechanism of collapse of the rebuilt dome.

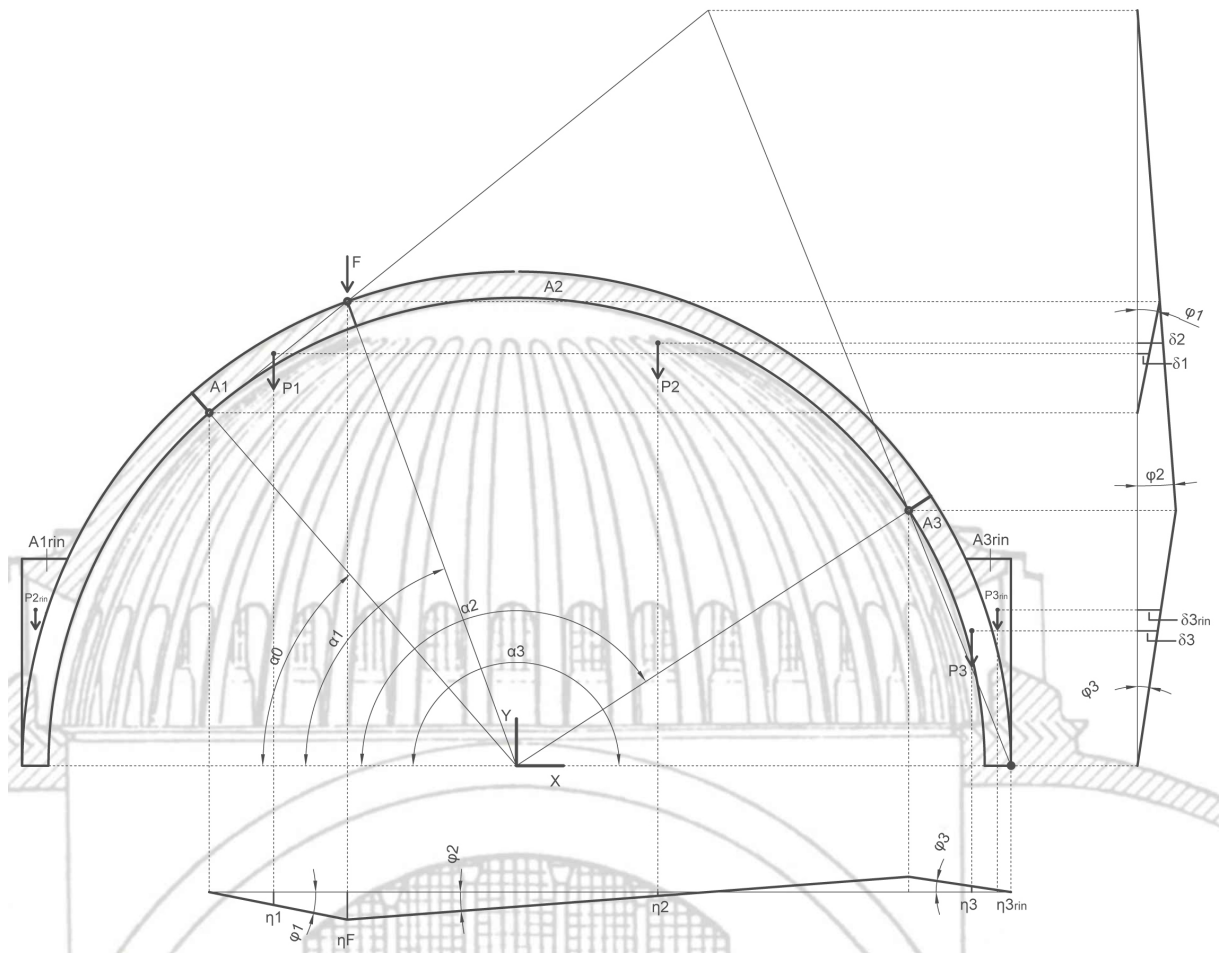


Fig. 24 – Hagia Sophia: mechanism of collapse taking into account the backfill.

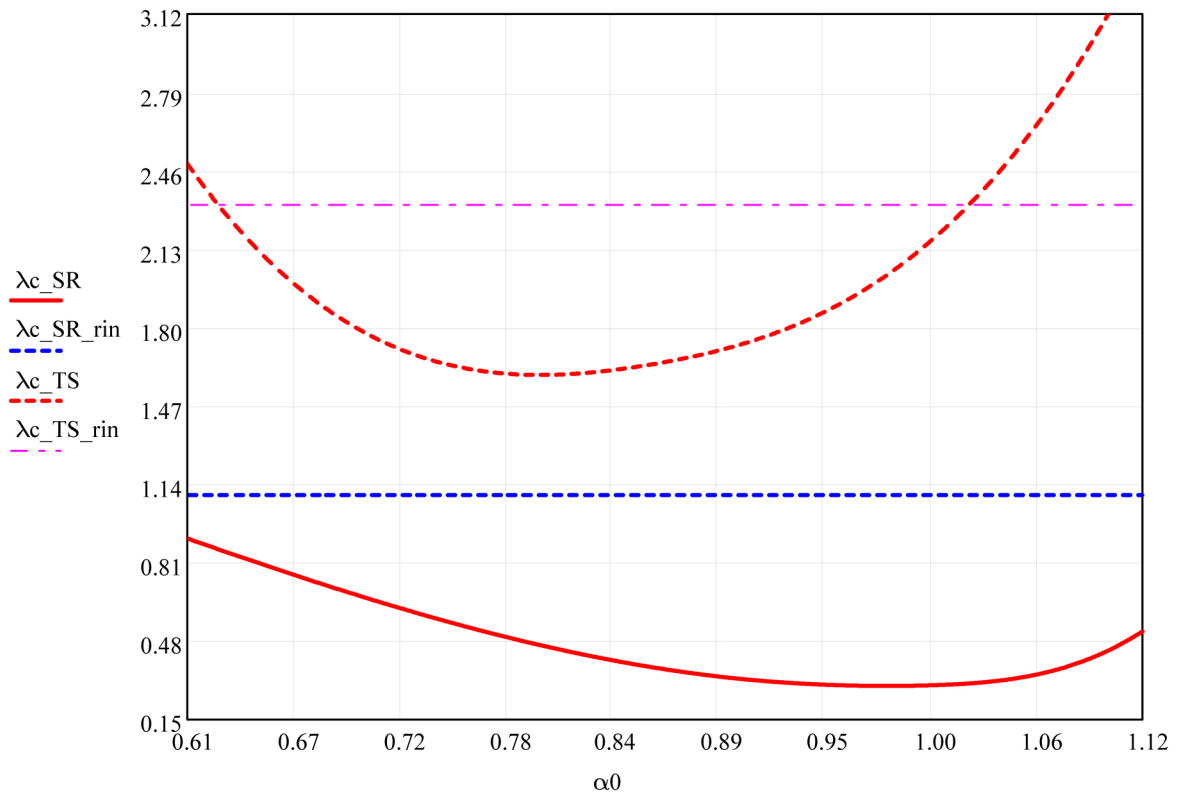


Fig. 25 – Hagia Sophia: comparison between the original and the rebuilt dome considering or not the backfill.

	α_0	α_1	α_2	α_3	α_4	X_1	Y_1	X_2	Y_2	X_3	Y_3	X_4	Y_4
0	0.000	1.238	1.903	α_2	π	-5.960	2.630	2.248	9.133	1.944	8.264	6.880	2.630
1	0.124			2.027		-5.914	3.367			2.626	7.980		
2	0.248			2.151		-5.778	4.093			3.267	7.615		
3	0.372			2.275		-5.552	4.796			3.859	7.172		
4	0.496			2.399		-5.242	5.466			4.391	6.660		
5	0.620			2.523		-4.851	6.093			4.856	6.086		
6	0.744			2.647		-4.385	6.666			5.246	5.459		
7	0.868			2.771		-3.852	7.178			5.555	4.789		
8	0.992			2.895		-3.26	7.619			5.780	4.085		
9	1.116			3.019		-2.618	7.984			5.915	3.359		
10	α_1		α_4		-1.947	8.263			5.960	2.630			

	X_{G1}	Y_{G1}	X_{G2}	Y_{G2}	X_{G3}	Y_{G3}	X_{2ass}	η_1	η_2	η_3	η_{F1}	η_{F2}	λ_c
0	-4.910	6.128	0	2.630	4.908	4.814	1.619	-1.05	21.146	-1.693	-3.712	-8.204	-0.837
1	-4.742	6.473	2.468	8.564	5.180	4.543	1.903	-1.172	-13.393	-6.841	-3.667	-8.158	-2.768
2	-4.545	6.805	2.826	8.389	5.430	4.248	2.192	-1.233	-91.933	-62.617	-3.53	-8.021	-23.656
3	-4.319	7.122	3.167	8.185	5.656	3.931	2.472	-1.233	24.179	19.544	-3.305	-7.796	7.249
4	-4.067	7.421	3.489	7.954	5.856	3.595	2.721	-1.175	12.166	10.874	-2.994	-7.486	4.135
5	-3.789	7.700	3.791	7.698	6.029	3.241	2.906	-1.062	9.535	8.839	-2.603	-7.094	3.623
6	-3.488	7.955	4.068	7.419	6.172	2.873	2.969	-0.898	10.11	9.072	-2.138	-6.629	4.268
7	-3.165	8.186	4.321	7.120	6.285	2.493	2.784	-0.687	17.469	14.158	-1.605	-6.096	8.243
8	-2.824	8.390	4.546	6.803	6.366	2.104	2.011	-0.437	-59.073	-41.028	-1.013	-5.504	-32.09
9	-2.466	8.565	4.743	6.470	6.415	1.709	-0.781	-0.152	-8.874	-5.187	-0.37	-4.862	-5.910
10	0	2.630	4.908	6.129	0	1.315	-29.121	-1.947	-4.55	-35.081	0.301	-4.191	-12.912

not variable data
 combination that provides minimum λ_c

Table 1 – Example of algorithm's calculation

	α_0	α_1	α_2	α_3	α_4	λ_c
General case	0.620	1.238	1.903	2.523	3.147	3.623
Hemispheric dome loaded by 2 forces	0.615	1.230	1.911	2.526	3.147	1.113
Hemispheric dome without lantern	0.569	1.222	2.428	3.147	/	0.186

Table 2 – Angles (rad) and minimum collapse multipliers of the different typologies of dome.

	α_0	α_1	α_2	α_3	α_4	λ_c
San Carlo alle Quattro Fontane: cross section	0.889	1.266	1.875	2.637	3.147	0.553
San Carlo alle Quattro Fontane: longitudinal section	0.620	1.238	1.903	2.523	3.147	3.623
Cathedral of Noto	0.815	1.353	1.789	2.600	3.147	0.149
Anime Sante: without backfill	0.788	1.313	1.827	2.615	3.147	0.077
Anime Sante: with backfill	0.788	1.313	1.827	2.615	3.147	0.302
Hagia Sophia: original dome	0.958	1.222	1.836	2.449	/	0.294
Hagia Sophia: original dome with backfill	0.958	1.222	1.836	2.449	/	1.095
Hagia Sophia: rebuilt dome	0.855	1.222	2.565	3.147	/	1.643
Hagia Sophia: rebuilt dome with backfill	0.855	1.222	2.565	3.147	/	2.317

Table 3 – Angles (rad) and minimum collapse multipliers of the different cases study.